



## Molecular Crystals and Liquid Crystals

Publication details, including instructions for authors and subscription information:

<http://www.tandfonline.com/loi/gmcl20>

### Influence of the Precursor Annealing on the Cu(In,Ga)Se<sub>2</sub> Solar Cell Performance

Hye-Jin Han<sup>a</sup>, Sang-Wook Park<sup>a</sup>, Soon-Rok Park<sup>a</sup>, Ju-Young Baek<sup>a</sup>,  
Tae-Young Yun<sup>a</sup>, Jun-Seong Park<sup>a</sup> & Chan-Wook Jeon<sup>a</sup>

<sup>a</sup> Optoelectronic Devices Laboratory, School of Chemical Engineering, Yeungnam University, Gyeongsan, Korea

Published online: 08 Jan 2014.

To cite this article: Hye-Jin Han, Sang-Wook Park, Soon-Rok Park, Ju-Young Baek, Tae-Young Yun, Jun-Seong Park & Chan-Wook Jeon (2013) Influence of the Precursor Annealing on the Cu(In,Ga)Se<sub>2</sub> Solar Cell Performance, Molecular Crystals and Liquid Crystals, 585:1, 145-152, DOI: [10.1080/15421406.2013.851371](https://doi.org/10.1080/15421406.2013.851371)

To link to this article: <http://dx.doi.org/10.1080/15421406.2013.851371>

PLEASE SCROLL DOWN FOR ARTICLE

Taylor & Francis makes every effort to ensure the accuracy of all the information (the "Content") contained in the publications on our platform. However, Taylor & Francis, our agents, and our licensors make no representations or warranties whatsoever as to the accuracy, completeness, or suitability for any purpose of the Content. Any opinions and views expressed in this publication are the opinions and views of the authors, and are not the views of or endorsed by Taylor & Francis. The accuracy of the Content should not be relied upon and should be independently verified with primary sources of information. Taylor and Francis shall not be liable for any losses, actions, claims, proceedings, demands, costs, expenses, damages, and other liabilities whatsoever or howsoever caused arising directly or indirectly in connection with, in relation to or arising out of the use of the Content.

This article may be used for research, teaching, and private study purposes. Any substantial or systematic reproduction, redistribution, reselling, loan, sub-licensing, systematic supply, or distribution in any form to anyone is expressly forbidden. Terms & Conditions of access and use can be found at <http://www.tandfonline.com/page/terms-and-conditions>

## Influence of the Precursor Annealing on the Cu(In,Ga)Se<sub>2</sub> Solar Cell Performance

HYE-JIN HAN, SANG-WOOK PARK, SOON-ROK PARK,  
JU-YOUNG BAEK, TAE-YOUNG YUN, JUN-SEONG PARK,  
AND CHAN-WOOK JEON\*

Optoelectronic Devices Laboratory, School of Chemical Engineering, Yeungnam University, Gyeongsan, Korea

*The stacked CuGa/In metallic precursor thin films were fabricated and annealed at low temperature of 200°C before the selenization for fabricating Cu(In,Ga)Se<sub>2</sub> photovoltaic absorber. The pre-annealing of Cu-In-Ga precursor was found to reduce Cu<sub>9</sub>Ga<sub>4</sub> phase and increase the formation of Cu<sub>16</sub>(In,Ga)<sub>9</sub> phase, which may be preferable for the subsequent selenization in terms of homogenizing Ga across the absorber thickness. However, the replacement of In with Ga in the ternary phase produced large amount of free-In, which gave rise to blistered area as shunt paths after the selenization. The performance of solar cell fabricated using the pre-annealed precursor was heavily deteriorated compared to the not-annealed precursor.*

**Keywords** Two-step process; selenization; Cu-In-Ga precursor; precursor annealing

### Introduction

Cu(In,Ga)Se<sub>2</sub> (CIGS)-based thin film solar cell has already been partially commercialized due to its high cell efficiency. CIGS thin film solar cells exhibit an efficiency of 20% at a laboratory scale, which is the highest efficiency ever reported for any kind of thin film solar cells [1]. Cu(In,Ga)Se<sub>2</sub> as a thin film photovoltaic absorption layer, is generally made using either co-evaporation of four elements onto a heated substrate or the two step process of Cu-In-Ga metal precursor sputtering followed by selenization. The highest efficiency was obtained by the three stage co-evaporation process developed by NREL. Since this technique does not guarantee a good stoichiometry over a large area, now most research is oriented towards processes that are easily scalable and that are able to produce low cost and efficient modules. The two step process is expected to allow a better yield management for large area module [2]. However, as one of the drawbacks, the two step process has such an inherent problem that Ga, which is alloyed to increase the bandgap energy of the absorber, is crowded near Mo back contact during the selenization process. This happens due to the reaction rate difference of In and Ga with Se; In forms its selenide much faster than Ga. The crowded Ga sometimes leaves a metallic phase of Cu<sub>9</sub>Ga<sub>4</sub> right on the Mo surface, which suggest that the phase is quite resistant against the selenization reaction

---

\*Address correspondence to Prof. Chan-Wook Jeon, Department of Chemical Engineering, Yeungnam University, Dae-dong, Gyeongsan-si, Gyeongbuk, 712-749, Korea (ROK). Tel: +8253-810-3860; Fax: +8253-810-4631. E-mail: cwjeon@ynu.ac.kr

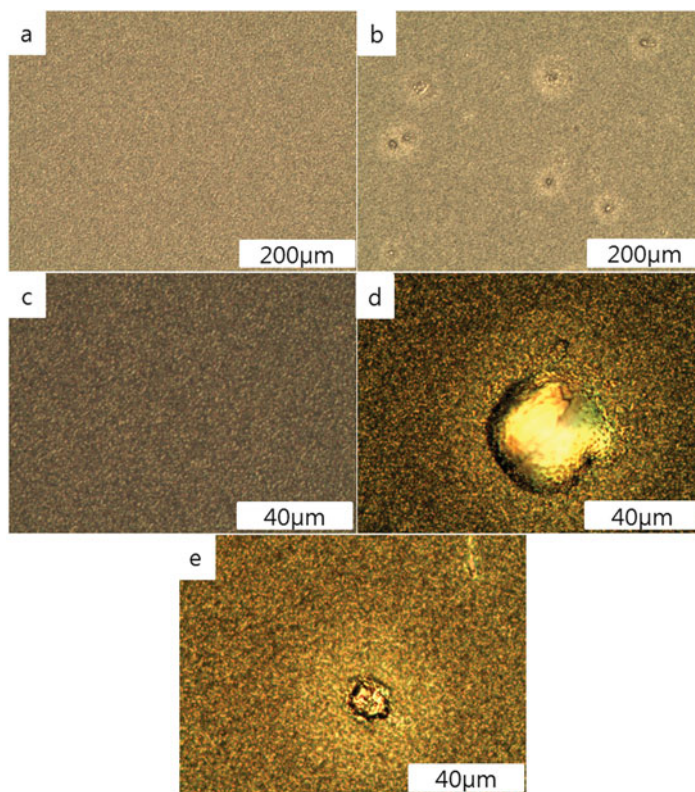


**Figure 1.** Optical micrographic images of precursor obtained from (a) and (c) the not-annealed precursors, (b), (d), and (e) the annealed precursors.

[3, 4]. Including the  $\text{Cu}_9\text{Ga}_4$  phase, in the middle of the selenization reaction, the precursor film would contain various metallic phases like  $\text{Cu}_2\text{In}$  (or  $\text{Cu}_{16}\text{In}_9$ ),  $\text{Cu}_{11}\text{In}_9$  and pure In as well [5, 6]. Among these, the  $\text{Cu}_{16}\text{In}_9$  phase is known to incorporate more Ga during the ramp-up for selenization reaction [7]. It would be highly desirable to mix all the three elements of Cu, In, and Ga, that is, such as the ternary phase of  $\text{Cu}_{16}(\text{In,Ga})_9$ , in terms of precursor homogenization.

In this study, the precursor annealing before the selenization process was carried out in an effort to homogenize Ga distribution across the precursor thickness by promoting the  $\text{Cu}_{16}(\text{In,Ga})_9$  ternary alloy phase. Nevertheless, surface morphology of the annealed precursor was found to become worse. Therefore, we investigated the influences of the precursor morphology on the selenization process and the solar cell performance.

## Experimental

The  $\text{Cu}(\text{In,Ga})$  precursor films were deposited on  $0.6 \mu\text{m}$  thick Mo coated soda-lime glass substrates using a DC-magnetron sputtering system. A CuGa (28at% Ga) alloy target and pure In target were selected as main sources. The precursor films consist of three sequential CuGa/In layers, where each pair of CuGa/In has identical thickness of roughly 200 nm.

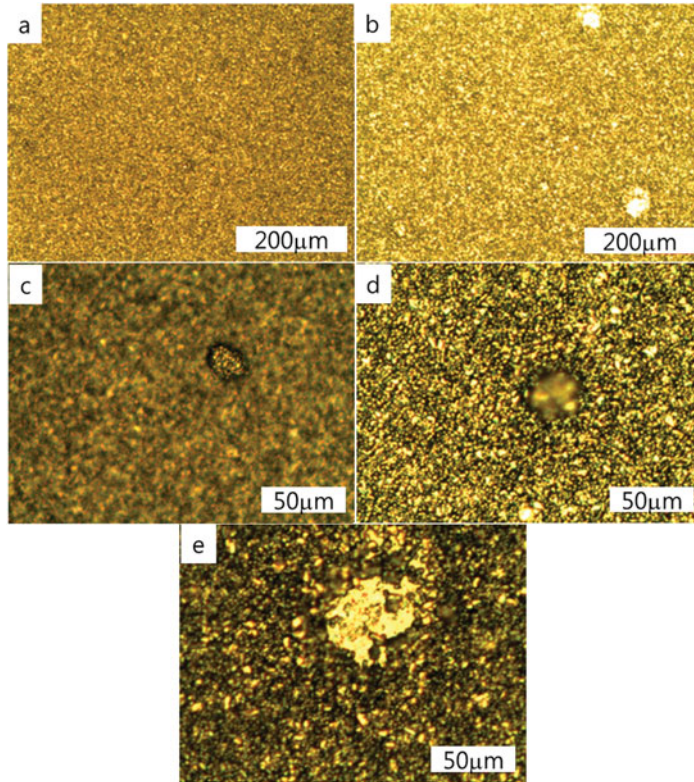


**Figure 2.** Optical micrographic images of CIGS thin films obtained from (a) and (c) the not-annealed precursors, (b), (d) and (e) the annealed precursors.

The composition of the precursors were adjusted to give  $\text{Cu}/(\text{In}+\text{Ga}) \sim 0.85$  by changing the sputtering duration of each target. This multilayer structure should ensure a good intermixture of the components. One of the prepared precursors was annealed at  $200^\circ\text{C}$  for 15 min by halogen ramp under vacuum. And another was not annealed.

The solid state selenization of the precursors was carried out in a resistively heated quartz furnace with  $\text{N}_2$  atmosphere of 1 atm for 20 min at  $460\sim 500^\circ\text{C}$ . Subsequently, CdS buffer layer was grown by chemical bath deposition (CBD) and window layer of un-doped ZnO (80 nm) and Al-doped ZnO (500 nm) was deposited via a RF-magnetron sputtering and DC-magnetron sputtering, respectively.

## Measurements

The surface morphologies of the precursor and the selenized layer were analyzed by optical microscope and charge-coupled device (CCD). X-ray diffraction (XRD) measurements were carried out at RT with a Cu anode X-ray tube in a  $\Theta-2\Theta$  measurement setup. The Mo(110) reflection at  $2\Theta = 40.5^\circ$  was used as reference to correct the x-ray beam alignment. The evaluation of photovoltaic performance of the solar cells has been performed using solar simulator under AM1.5,  $100 \text{ mW}/\text{cm}^2$  illumination at  $25^\circ\text{C}$ .

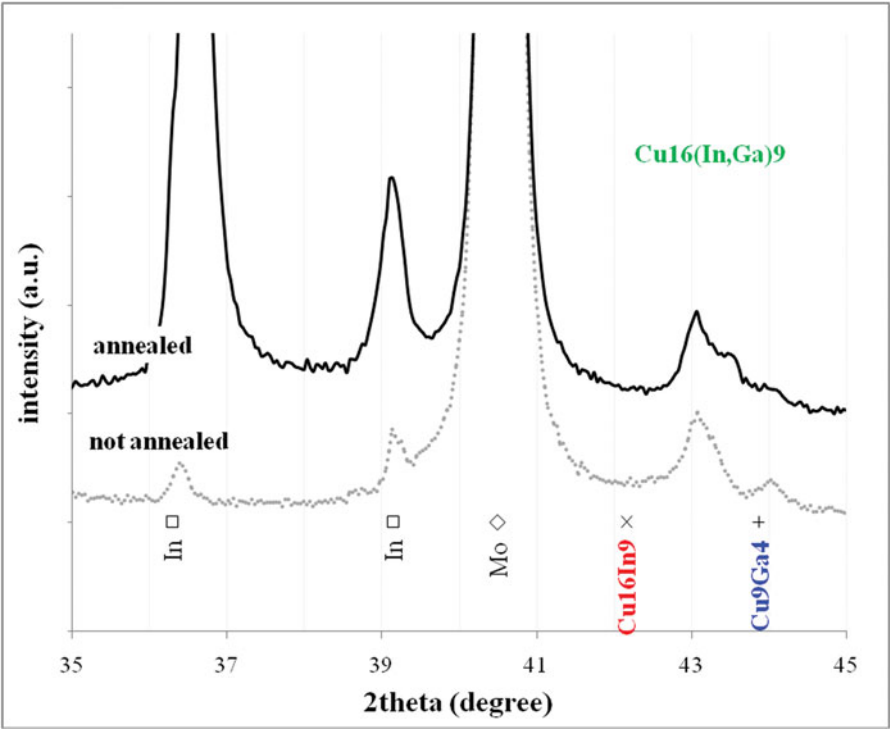


Figure 3. Diffractogram of samples with the annealed and not-annealed precursors.

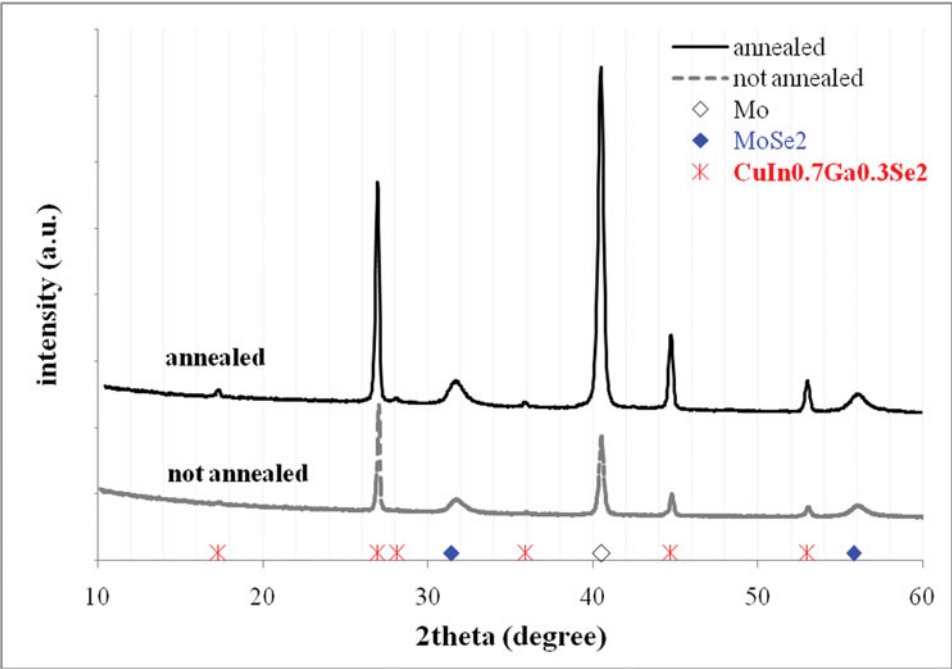
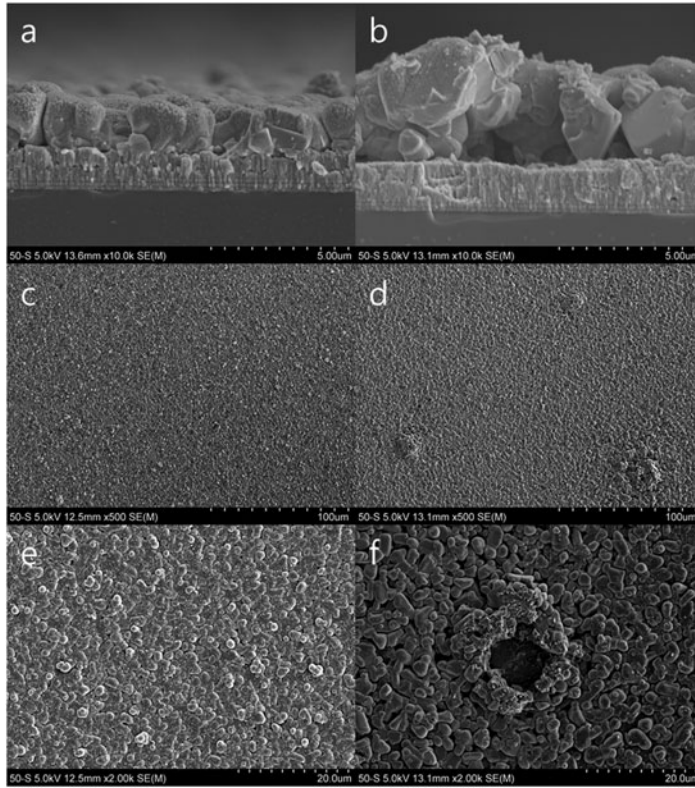


Figure 4. Diffractogram of samples with the annealed and not-annealed CIGS thin films.



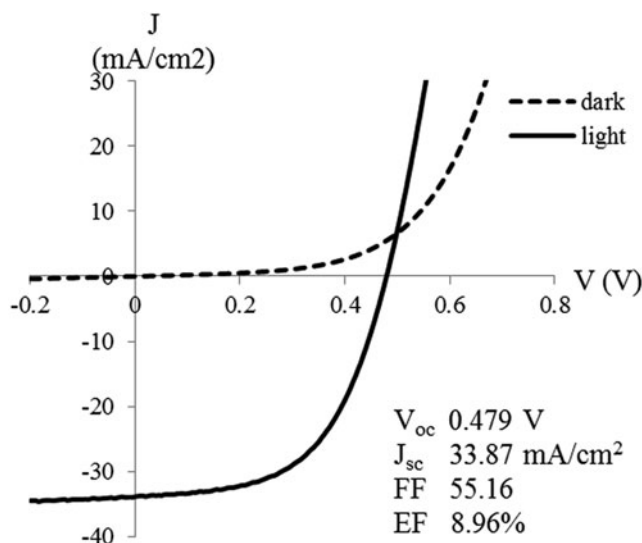
**Figure 5.** Cross-sectional views of the CIGS thin films with (a) not-annealed precursor and (b) annealed precursor, plane views of them with (c) and (e) not-annealed precursor and (d) and (f) annealed precursor.

## Results and Discussion

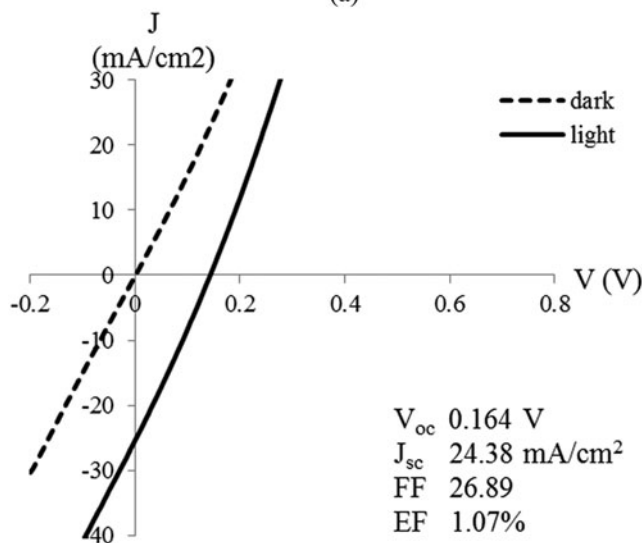
The morphologies of the CIGS absorber layers selenized from the annealed and not-annealed precursors are shown in Fig. 1 and Fig. 2. The annealed precursor (Fig. 1b) shows lots of bumps with size distribution, which is absent on the not-annealed precursor surface (Fig. 1a). Some of the bumps are very large in size and looks metallic shiny (hereafter “big bump”), which presumably are In droplets or In-enriched alloy phases (Fig. 1d). The other small bumps (hereafter “small bump”) shown in Fig. 1e are also assumed to be In-bumps. The free-In would be released and agglomerated to form a bump since the precursor itself is In-rich and also In-rich alloy phases are not allowed as far as the precursor film was made by sputtering.

The bumps of similar shape are found even after the selenization of the precursors as shown in Fig. 2. They are not likely free-In (or In-rich metallic alloy) since indium selenide forms far below the selenization temperature of 530°C, however, obviously related with the In-bumps found in the precursor surface [8]. Fig. 2e is an example of the burst In-bump, which is highly likely matching to the big bump of the precursor. In the center of the blistered area, the back contact Mo surface was exposed, which can provide with a shunt path for the solar cell [9].





(a)



(b)

**Figure 6.** J-V curve of thin film solar cells. (a) Not-annealed precursor solar cell J-V curve (b) Annealed precursor solar cell J-V curve.

As shown Fig. 3, XRD patterns of the annealed and not-annealed precursors were compared. For the not annealed precursor, the reflection positions of  $\text{Cu}_9\text{Ga}_4$  (PDF# 71-0458) phases are clearly separated from the ternary  $\text{Cu}_{16}(\text{In,Ga})_9$ , which is shifted towards higher angle by incorporating more Ga compared to  $\text{Cu}_{16}\text{In}_9$  (PDF#42-1475) [5, 6]. For the annealed precursor, however,  $\text{Cu}_9\text{Ga}_4$  peak disappeared and a new peak, which can be indexed as  $\text{Cu}_{16}(\text{In,Ga})_9$  phase but having even greater Ga content than the original one, emerged between the two binary peaks. This result suggests that Ga is released from  $\text{Cu}_9\text{Ga}_4$  and replace In of the ternary phase, which makes the free-In peak intensity stronger. The big

bumps in the annealed precursor observed in the microscope image of Fig. 1d, is well consistent with the XRD patterns.

Figure 4 shows the XRD patterns of the selenized layers of the two precursors. Both films are well matched to the  $\text{CuIn}_{0.7}\text{Ga}_{0.3}\text{Se}_2$  phase and no other secondary phase was found except  $\text{MoSe}_2$ . Qualitatively, the crystalline quality of CIGS obtained from the annealed precursor seems to be better than the not-annealed precursor when comparing the diffraction intensity. Also, the annealed precursor resulted in weaker peak intensity of  $\text{MoSe}_2$ , telling that the pre-annealing of metal precursor suppresses the excessive formation of  $\text{MoSe}_2$  phase.

Figure 5 shows the cross-section and plan view SEM images of both CIGS's. As expected from the XRD analysis, it can be clearly observed that the grain size of CIGS and the  $\text{MoSe}_2$  thickness are much greater for the annealed precursor (Fig. 5a and 5b). The bump distribution is well consistent with the previous optical microscope results as shown Fig. 5c and 5d. Fig. 5b and 5c correspond to the blistered area found after the selenization. At the moment, the formation mechanism of the blistering is not clear, however, it is obvious that the big In bump is closely relevant such that In diffuses faster away from the bump than Cu heading towards the bump center, which will deplete material and form a void. Anyway, there is a high chance for a shunt path due to the exposed Mo back contact.

Figure 6 shows the current-voltage characteristics of two CIGS solar cells with different precursor annealing history. The annealed precursor yielded a heavily shunted diode behavior. It is apparent that the abnormal I-V behavior stems from the blistered area.

## Conclusions

The precursor annealing before the selenization process was carried out in an effort to homogenize Ga distribution by promoting the Cu-Ga-In ternary alloy phase [10, 11]. However, the surface morphology of the annealed precursor was found to become worse mainly due to the formation of big In bumps. This study successfully demonstrated that the precursor annealing process can incorporate more Ga in  $\text{Cu}_{16}(\text{In,Ga})_9$  phase and thus uniform Ga distribution across the film thickness. However the In substituted by Ga came out and clustered on the surface. Some of the In bumps were blistered after the selenization reaction and provided a high density of shunt paths, which manifested by the nearly shorted I-V behavior.

## Acknowledgment

This research was financially supported by the Ministry of Education, Science Technology (MEST) and National Research Foundation of Korea (NRF) through the Human Resource Training Project for Regional Innovation. This work was supported by the New & Renewable Energy of the Korea Institute of Energy Technology Evaluation and Planning (KETEP) grant funded by the Korea government Ministry of Knowledge Economy.(No. 20123010010130)

## Reference

- [1] Stanbery, B. J. (2002). *Critical Reviews in Solid State and Materials Sciences.*, 27, 73–117.
- [2] Niki, S., Contreras, M., Repins, I., Powalla, M., Kushiya, K., Ishizuka, S., & Matsubara, K. (2010). *Progress in Photovoltaics: Research and Applications.*, 18, 453.



- [3] Hanket, G. M., Shafarman, W. N., McCandless, B. E., & Birkmire, R. W. (2007). *J. Appl. Phys.*, 102, 074922–074922.
- [4] Hanket, G. M., Shafarman, W. N., & Birkmire, R. W. (2006). *IEEE Photovoltaic Energy Conversion*, 1, 560–563.
- [5] Purwins, M., Enderle, R., Schmid, M., Berwian, P., Muller, G., Hergert, F., Jost, S., & Hock, R. (2007). *Thin Solid Films*, 515, 5895–5898.
- [6] Brummer, A., Honkimaki, V., Berwian, P., Probst, V., alm, J. P., & Hock, R. (2003). *Thin Solid Films*, 437, 297–307.
- [7] Holzing, A., Schurr, R., Jost, S., Palm, J., Deseler, K., Wellmann, P., & Hock, R. (2011). *Thin Solid Films*, 519, 7197–7200.
- [8] Hergert, F., Hock, R., Weber, A., Purwins, M., Palm, J., & Probst, V. (2005). *Journal of Physics and Chemistry of Solids*, 66, 1903–1907.
- [9] Dhere, N. G., Kuttath, S., & Moutinho, H. R. (1995). *J. Vac. Sci. Technol.*, 13, 1078–1082.
- [10] Song, H. K., Jeong, J. K., Kim, H. J., Kim, S. K., & Yoon, K. H. (2003). *Thin Solid Films*, 435, 186–192.
- [11] Jiang, F., & Feng, J. (2006). *Thin Solid Films*, 515, 1950–1955.